

Slow Covariations in Neuronal Resting Potentials Can Lead to Artefactually Fast Cross-Correlations in Their Spike Trains

CARLOS D. BRODY

Instituto de Fisiología Celular, Universidad Nacional Autónoma de México, C.P. 04510 México D.F., Mexico

Brody, Carlos D. Slow covariations in neuronal resting potentials can lead to artefactually fast cross-correlations in their spike trains. *J. Neurophysiol.* 80: 3345–3351, 1998. A model of two lateral geniculate nucleus (LGN) cells, which interact only through slow (tens of seconds) covariations in their resting membrane potentials, is used here to investigate the effect of such covariations on cross-correlograms taken during stimulus-driven conditions. Despite the slow timescale of the interactions, the model generates cross-correlograms with peak widths in the range of 25–200 ms. These bear a striking resemblance to those reported in studies of LGN cells by Sillito et al., which were taken at the time as evidence of a fast spike timing synchronization interaction; the model highlights the possibility that those correlogram peaks may have been caused by a mechanism other than spike synchronization. Slow resting potential covariations are suggested instead as the dominant generating mechanism. How can a slow interaction generate covariogram peaks with a width 100–1,000 times thinner than its timescale? Broad peaks caused by slow interactions are modulated by the cells' poststimulus time histograms (PSTHs). When the PSTHs have thin peaks (e.g., tens of milliseconds), the cross-correlogram peaks generated by slow interactions will also be thin; such peaks are easily misinterpretable as being caused by fast interactions. Although this point is explored here in the context of LGN recordings, it is a general point and applies elsewhere. When cross-correlogram peak widths are of the same order of magnitude as PSTH peak widths, experiments designed to reveal short-timescale interactions must be interpreted with the issue of possible contributions from slower interactions in mind.

INTRODUCTION

A model of two lateral geniculate nucleus (LGN) cells is used here to investigate the effect of slow resting potential covariations on spike train correlograms taken during stimulus-driven conditions. The slow covariations used have a timescale of tens of seconds, and no other interaction between the cells is present in the model. Despite the slow timescale of the interaction, the model generates covariogram peaks remarkably similar to those reported in studies of LGN cells by Sillito et al. (1994), which had typical widths in the range of 25–200 ms and which were interpreted, based on their widths, as evidence of a fast spike timing synchronization. The results show that such widths can be obtained even in the absence of a fast spike timing synchronization and suggest that the covariogram peaks of Sillito et

al. may have been caused by other mechanisms. In particular, slow resting membrane potential covariations (see Mukherjee et al. 1995) are suggested as the dominant generating mechanism.

All spike train correlograms will be assumed collected over many identically prepared trials of an experiment and corrected for coincidences expected by chance, given their two poststimulus time histograms (PSTHs), with the standard technique known as shuffle correction (Aertsen et al. 1989; Palm et al. 1988; Perkel et al. 1967). The name "shuffle-corrected cross-correlogram" will be abbreviated here to "covariogram."¹

Readers will at once ask, "how can an interaction with a timescale in the tens of seconds generate a covariogram peak with a width in the tens of milliseconds?" The explanation is not specific to LGN recordings. In brief it is the following. A positive peak in a spike train covariogram indicates that there are parameters that are covarying in the two neurons. However, the covarying parameters may be internal ones, and the spike trains allow us (indirect) access to them only while the neurons are firing; when one or both of the neurons are not firing, we have no way of knowing whether internal parameters are still covarying. During such zero-firing times the covariogram is constrained to be zero. Therefore the width of the covariogram peak is a function not only of the timescale and kind of interaction but also of the PSTHs of the two neurons, because the PSTHs indicate when the neurons fire and when they don't. This effect becomes important when the timescale of interaction is comparable with, or greater than, the timescale of variations in the PSTHs (Brody 1997): The PSTHs will then modulate what would otherwise be a broad correlogram peak. In particular, when the interactions are slow, thin PSTHs will necessarily lead to thin covariogram peaks. Thus, if a covariogram peak width is of the same order of magnitude as the PSTH peak widths, investigators should be careful to check for other, slow, interactions before concluding that the covariogram peak is due to spike synchronization. See Brody (1988a) for an expanded treatment of this point, and see Friston (1995) and Brody (1998b) for methods to distinguish spike synchronization interactions from other types of interactions. This paper, together with that of Brody (1997), is an example of such a check, applied to the results of Sillito et al.

The costs of publication of this article were defrayed in part by the payment of page charges. The article must therefore be hereby marked "advertisement" in accordance with 18 U.S.C. Section 1734 solely to indicate this fact.

¹ The abbreviation covariogram comes from the fact that the computation of the shuffle-corrected cross-correlogram is exactly analogous to the computation of covariance when the variables of interest are scalars rather than spike trains (Aertsen et al. 1989; Brody 1998a).

METHODS

Following Mukherjee and Kaplan (1995), a five-channel, Hodgkin-Huxley style, simplified version of McCormick and Huguenard's single-compartment model of geniculate cells (Huguenard and McCormick 1992; McCormick and Huguenard 1992) was used here. This is a simple model that was nevertheless established to reproduce major features of geniculate cell firing. There are five channels in the model: 1) a low-threshold Ca^{2+} channel, the inactivation of deinactivation of which is determined by the membrane resting potential and which controls whether the cell responds to depolarizing input with tonic firing or with a burst of Na^+ spikes riding on a slow Ca^{2+} spike (Jahnsen and Llinas 1984; McCormick and Huguenard 1992; Mukherjee and Kaplan 1995); 2) a transient Na^+ and 3) a delayed rectifier K^+ channel that generate action potentials; 4) a leak Na^+ and 5) a leak K^+ conductance that set the membrane resting potential. On each trial, the two cells' membrane voltages were recorded, and upward crossings above a -25 mV threshold were taken as spike initiation times. The resulting spike trains from many such trials were then used to compute covariograms.

Two types of synaptic connectivities were used. In the first (the main model) the only ionotropic synaptic inputs to the two LGN cells were those from retinal ganglion cells (RGCs). Each LGN cell received input from a single, separate, RGC. Spike times for the model RGCs were taken from extracellular recordings by J. M. Alonso and R. C. Reid (unpublished observations) of a typical RGC in an anesthetized cat, stimulated by drifting sine wave gratings—a condition similar to that used in the experiments of Sillito et al. (1994). RGC spike times in response to $\sim 3,000$ modulations of a drifting sine-wave grating were available to be used as inputs for the model. Different trials used as input different modulations from the RGC spiking data. In the model, each incoming RGC spike generated a conductance change in the cell with an α -function-shaped waveform

$$g_{\text{ampa}} = \hat{g}_{\text{ampa}}[(t - t_0)/\tau]e^{-(t-t_0-\tau)/\tau} \quad \text{for } t \geq t_0, \quad 0 \text{ otherwise} \quad (1)$$

$$I_{\text{ampa}} = g_{\text{ampa}}(E_{\text{ampa}} - V_m) \quad (2)$$

Here t_0 is the arrival time of the spike, τ was set to 0.5 ms, \hat{g}_{ampa} was set to 27 nS, and E_{ampa} was set to +40 mV (similar to Mukherjee and Kaplan 1995). The effect of multiple incoming spikes on the conductance was additive. To contrast the effects of fast timescale interactions with the slow timescale interactions of the main model, a second type of synaptic connectivity was used in some runs. In this variant the two LGN cells received, in addition to their separate RGC inputs, ionotropic synaptic input from a common source. The spike source of the common input was a Poisson process with a time-varying rate that had a temporal waveform similar to the PSTH of the RGC inputs and a peak firing rate of 50 Hz. The maximum conductance of the common input was set to 16 nS.

The equations describing the model were numerically integrated with semi-implicit backward Euler integration with an adaptive timestep (Press et al. 1992); a single-compartment simulator program to do this was written in MATLAB 5. Information on how to obtain the simulator and the scripts detailing the simulations, to reproduce the results in their entirety, is given at the end of the paper.

RESULTS

Some features of single-cell LGN responses, necessary for understanding the origin of the covariogram shapes

shown later are illustrated in Fig. 1. The well-known difference between tonic firing at depolarized resting potentials (when low-threshold Ca^{2+} channels are inactivated) and burst firing at more hyperpolarized resting potentials (when the Ca^{2+} channels are deinactivated) (Jahnsen and Llinas 1984; McCormick and Huguenard 1992; Mukherjee and Kaplan 1995) is illustrated by the membrane potential traces shown in Fig. 1, *A* and *B*. The RGC input spikes shown are those produced by a real RGC, in response to a single bar of a luminance sine-wave grating drifting over the cell's receptive field. The rasters of Fig. 1C show, in finer voltage steps, how the LGN cell's firing changes between the two modes as a function of resting membrane potential. The crucial points to notice here are that 1) there is a tonic regime (≈ -52 to -70 mV), within which resting potential controls both response latency and "excitability" (i.e., number of spikes fired in response to a given input); 2) there is a burst regime (≈ -78 to -87 mV), within which the resting potential controls mostly the latency of the stereotyped burst response; and 3) the resting potential controls the transitions between these regimes.

The responses of two separate LGN cells to many trials of stimulation with drifting luminance sine-wave gratings were simulated. On each trial, the resting membrane potential of each cell was set by controlling its leak K^+ conductance. This resting potential was held constant during the trial and varied slowly over different trials. Apart from any interaction through their resting potentials (e.g., when the two resting potentials were set to covary over trials), the simulations of the two cells were independent and used independent inputs.

If the resting membrane potentials of the two cells covary, there is an interaction between them—the two cells are not behaving independently—and the covariogram of their spike trains will have a positive peak, although their interaction is not due to spike timing synchronization. Figure 2, *A1* and *A2*, illustrate this for the purely bursting case. The shape of the covariogram peak will depend on which firing regimes the cells participated in. The lower one-half of Fig. 2 illustrates three shapes caused by covarying resting potentials. They may be directly compared with the results reported in Sillito et al. (1994). In the first example, in Fig. 2, *D1* and *D2*, the cells remain always in the tonic or near-tonic regime; their resting potential varies from -74 to -56 mV. Notable features of the covariogram include the width of the peak and the fact that the covariogram curve is always above zero. An experimentally obtained covariogram with very similar features may be found in Fig. 2*a* of Sillito et al. (1994); the width and always-positive value of that covariogram are well reproduced in Fig. 2*D2*. The next example, in Fig. 2, *E1* and *E2*, shows two cells, which for the most part remain in the burst regime, below -78 mV. The most important component of their covariation is thus in the latency of their responses. This latency type of covariation leads to a peak surrounded by inhibitory dips (Brody 1997, 1998a). The width of the peak in Fig. 2*E2* is largely determined by the width of the bursts and is thus on the order of 20–30 ms. The covariogram in Fig. 2*E2* may be compared with Fig. 2*e* of Sillito et al. (1994), where a peak with a similar width, also surrounded by slight inhibitory dips, can be found. The

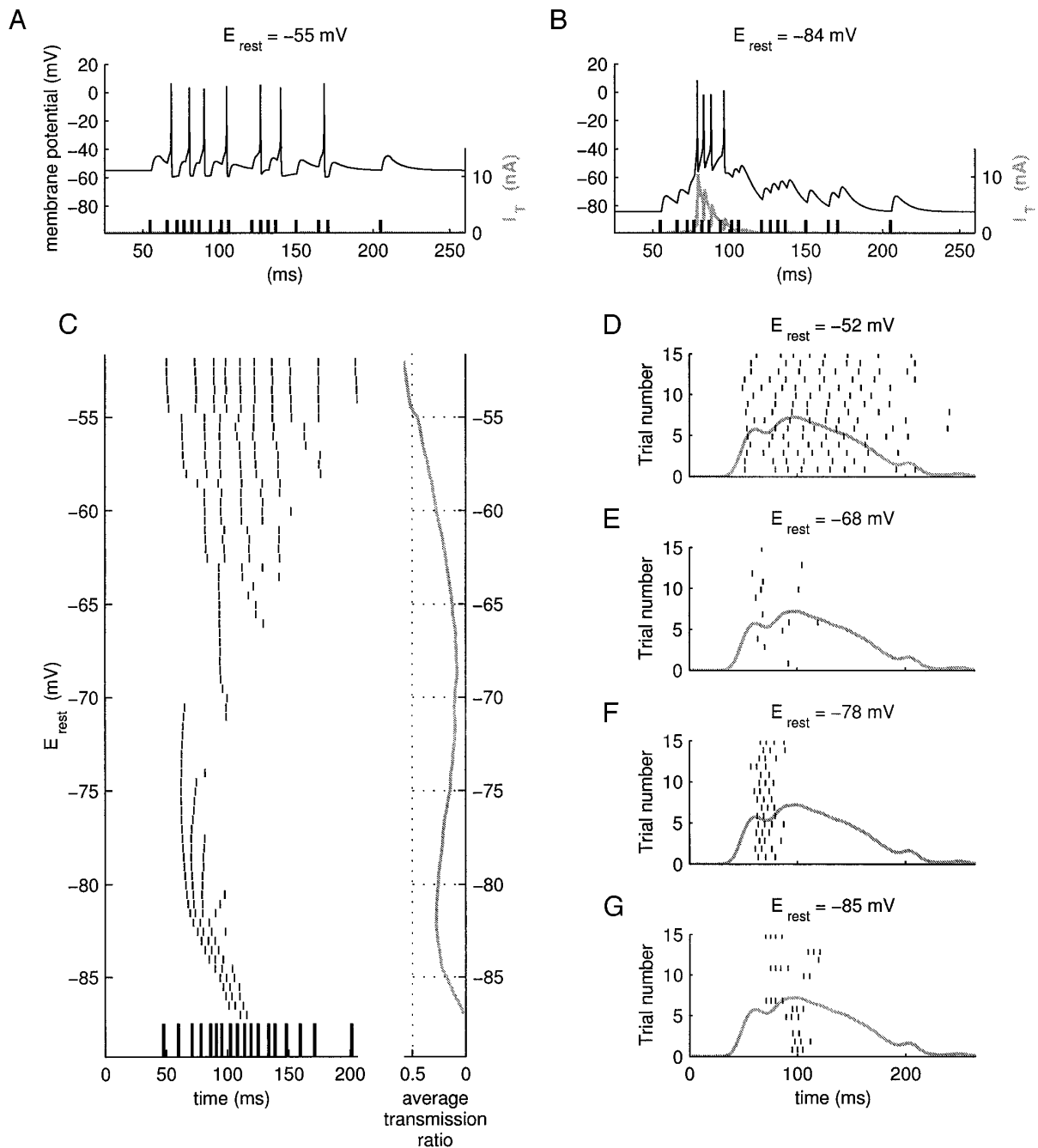


FIG. 1. *A* and *B*: traces of a model LGN cell's membrane voltage in response to retinal ganglion cell (RGC) input spikes (which are shown at the bottom as thick black lines). The panels illustrate tonic (*A*) vs. burst (*B*) responses. The low-threshold Ca^{2+} current is shown in gray and has its scale axis on the right. These 2 panels follow Fig. 11 of Mukherjee and Kaplan (1995). (The transmission ratio in *A* is high but not near 1 because of the short interspike intervals in the RGC spike train.) *C*: rasters of spike responses of the model as a function of resting membrane potential. Each row represents a different trial, run at the resting potential indicated at the left. The same RGC input train was used for all these trials; it is shown as thick black lines at the bottom. On the right is the transmission ratio (number of inputs spike/number of output spikes), averaged over many different RGC input trains. *D*–*G*: responses to 15 different RGC input trains, all at a particular, fixed E_{rest} . The thick gray line underlying the rasters is the poststimulus time histogram (PSTH) of the RGC input; its maximum value is 140 Hz. The LGN spikes' PSTH (not shown) in *D* is close to a scaled version of the RGC's PSTH. This is in contrast to *E*–*G*, where RGC and LGN PSTHs have very different shapes.

third and final example in the lower one-half of Fig. 2 is unlike the others in that the resting potentials of the two cells were not set to be precisely the same on every trial;

although the two resting potentials covaried, they were not identical (see the right side of Fig. 2*F1*). One cell (shown in gray) was kept within the tonic regime, sometimes firing

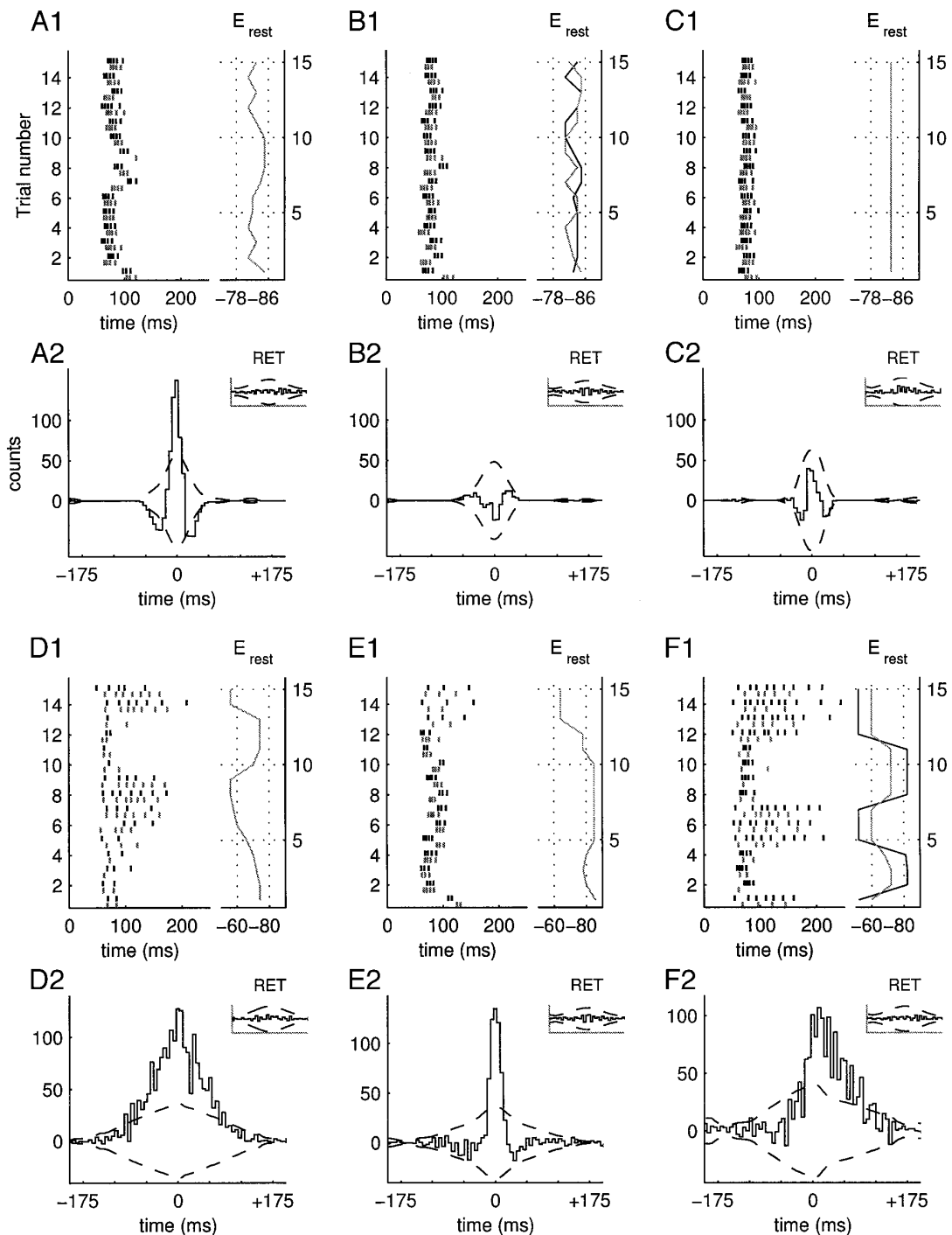


FIG. 2. Rasters and covariograms of 2 model LGN cells. Six example experiments are shown. *A1*, *B1*, *C1*, *D1*, *E1*, and *F1*: 15 representative rasters of the 2 cells, 1 cell in gray, the other in black. To the right of the rasters is a trace (in mV) of the value of the resting membrane potential, E_{rest} , over the different trials. The panels immediately below each raster panel show the corresponding covariograms. Dashed lines are statistical significance limits. Small insets labeled RET are covariograms of the 2 sets of RGC spike trains used as input to the LGN cells; these insets confirm that any significant peaks appear at the geniculate, not the retinal, level. Panel sets *A–C* focus on the purely bursting case. In panel *A1*, E_{rest} varied (within the burst regime) over trials and was the same for both cells in every trial. Thus the 2 cells had covarying resting potentials. *A2* shows the resulting covariogram peak (of a width similar to the PSTH width, not shown). In *B1*, the 2 resting potentials varied (again, within the burst regime), but did so independently of each other. In *C1*, the resting potentials stayed constant over all trials. Neither *B2* nor *C2* show a significant peak, which demonstrates that brief, bursty responses cannot alone account for the presence of the covariogram peak. Some covariation between the 2 cells is necessary. The bottom one-half of the figure, panel sets *D–F*, may be directly compared with the results of Sillito et al. (1994). See text for detailed commentary. In *D1* and *E1*, E_{rest} was the same for both cells in every trial; in *F1* the 2 cells had covarying, but not identical, resting potentials.

many spikes, sometimes very few at a longer latency. The second cell (shown in black) varied between firing tonically and firing in bursts. Because the two resting potentials covaried, there is a positive peak in the covariogram. However, because the two resting potentials were not varying between the same voltages, the two cells are not interchangeable and the peak is asymmetric. In Fig. 2*F2* there is slight dip to the left of zero, a sharp rise near zero, and a more gradual fall-off to the right of zero. This covariogram may be compared with Fig. 2*f* of Sillito et al. (1994), where the same asymmetric shape and slight dip to the left of zero can be found.

So far only the first 250 ms or so of the rasters of each trial were shown. The covariograms of Fig. 2 had their time axes clipped to ± 175 ms. However, in the model each trial lasted much longer than 250 ms; each trial was set to last 1,700–2,500 ms. With drifting gratings at temporal frequencies of 3 or 2 Hz, respectively, this is long enough for five bars of the grating to drift over the receptive fields. The resting membrane potentials were set to be constant during each entire trial, and to change either only gradually between trials, or only every three or four trials; if we assume an intertrial interval of a few seconds, these are then models of interactions with a timescale in the tens of seconds. Figure 3, *A* and *B*, shows the same covariograms as in Fig. 2, *D2* and *E2*, but with the covariogram window opened to its full extent (\pm the length of a trial), instead of clipped at ± 175 ms. The side peaks seen in Fig. 3, spaced with the periodicity of the stimulus, are indicative of the fact that the interactions between the two cells have a timescale longer than the temporal period of the drifting grating. When the covariograms are clipped to the ± 175 -ms window, only a single peak, which can be as narrow as 20 ms, is seen. This gives the false impression of a very short timescale interaction. Figure 3, *C1* and *C2*, shows, for comparison, a variant of the model where the resting potential of both cells was kept fixed at -60 mV throughout the whole simulation (thus avoiding slow resting-potential interactions), and in addition to the separate and independent RGC input the two cells received common, AMPA receptor-mediated synaptic input (leading to a fast interaction). In contrast to Fig. 3, *A* and *B*, no side peaks are observed. In Sillito et al. (1994), covariograms were clipped to ± 175 ms, as was done here in Fig. 2. However, side peaks with features similar to those shown in the model data, including the similarity of shape between side and central peaks, were found in all of the experimental data of Sillito et al. that was analyzed with a full covariogram window in (Brody 1997).

DISCUSSION

The modeling results show that, even in the absence of any synaptic or spike synchronizing interaction between two geniculate neurons, slow covariations in their resting potentials can generate narrow covariogram shapes remarkably similar to those reported by Sillito et al. (1994). The model also replicates most of their reported JPSTHs (Brody 1997). Covariations in LGN transmission ratios, presumably caused by covariations in resting membrane potentials, were observed previously (Mukherjee et al. 1995). Plausible mechanisms

that could cause covariations in resting membrane potentials are known, caused by both signals from cortex (which can activate metabotropic glutamate receptors) (Godwin et al. 1996; McCormick and von Krosigk 1992), and from the parabrachial region of the brain stem (which can activate metabotropic acetylcholine receptors) (Sherman and Guillery 1996; Uhrich et al. 1995). The timescale of these known mechanisms is in the tens of seconds, the same timescale as the interactions in the model described here. Thus the “covarying resting potentials hypothesis” may provide a simple and plausible explanation for much of the data reported in Sillito et al. (1994). Although simple, the explanation is powerful; a single model accounts for a multiplicity of covariogram shapes and explains the presence of both central and side peaks. (See note added in proof.) Because slow interactions could be caused by cortical input, the explanation is consistent with the covariogram peaks being induced by feedback from visual cortex. Sillito et al. (1994) reported that they observed covariogram peaks only between cells of like type (*X/Y ON/OFF*). If the interpretation proposed here were correct, this would suggest that there is a diffuse, but class-specific, control of resting potential in the LGN.

For anatomic reasons (Montero 1991; Murphy and Sillito 1996), short-timescale interactions, caused by common corticothalamic ionotropic synaptic input, may be expected in LGN cells. Most likely, the data of Sillito et al. contain contributions from both short and long timescale interactions. The results described here show that investigators wishing to follow the pioneering experiments of Sillito et al. (1994), and interested mostly in short timescale interactions, must take a number of precautions. First, the clearest signs of a common ionotropic input are likely to be available if experimenters control, during the experiment, for resting potential variations and attempt to keep these as steady as possible, preferably using only data from stable periods. Preliminary studies with the models described show that, unless the common ionotropic synaptic input is very strong, its presence is extremely difficult to detect if there are, in addition, resting potential covariations. Second, the full covariogram should always be shown, not just its central region. The presence of side peaks is a sure sign of slow interactions. Third, it can be seen in Fig. 2, *D1*, *E1*, and *F1*, that some of the rasters show, even to the human eye, symptoms of resting potential covariations (e.g., the firing rate covariations in panels *D1* and *F1* or the latency covariations in *E1*). Thus covariograms should always be shown together with examples of the rasters that generated them, allowing an opportunity to evaluate the plausibility of any accompanying covariogram interpretations. Finally, the issue of possible contributions to the covariogram from resting potential covariations or other interactions should always be explicitly addressed. In the absence of these precautions it is unfortunately impossible to take covariograms of LGN spike trains with shapes similar to those of Fig. 2 as conclusive evidence of spike timing synchronization.

Brody (1998a) describes some other warning signs, not specific to LGN recordings, that can alert investigators to the possibility of a peak being caused by interactions other than spike synchronization: 1) covariogram peak widths of the same order of magnitude as PSTH peak widths; 2) auto-

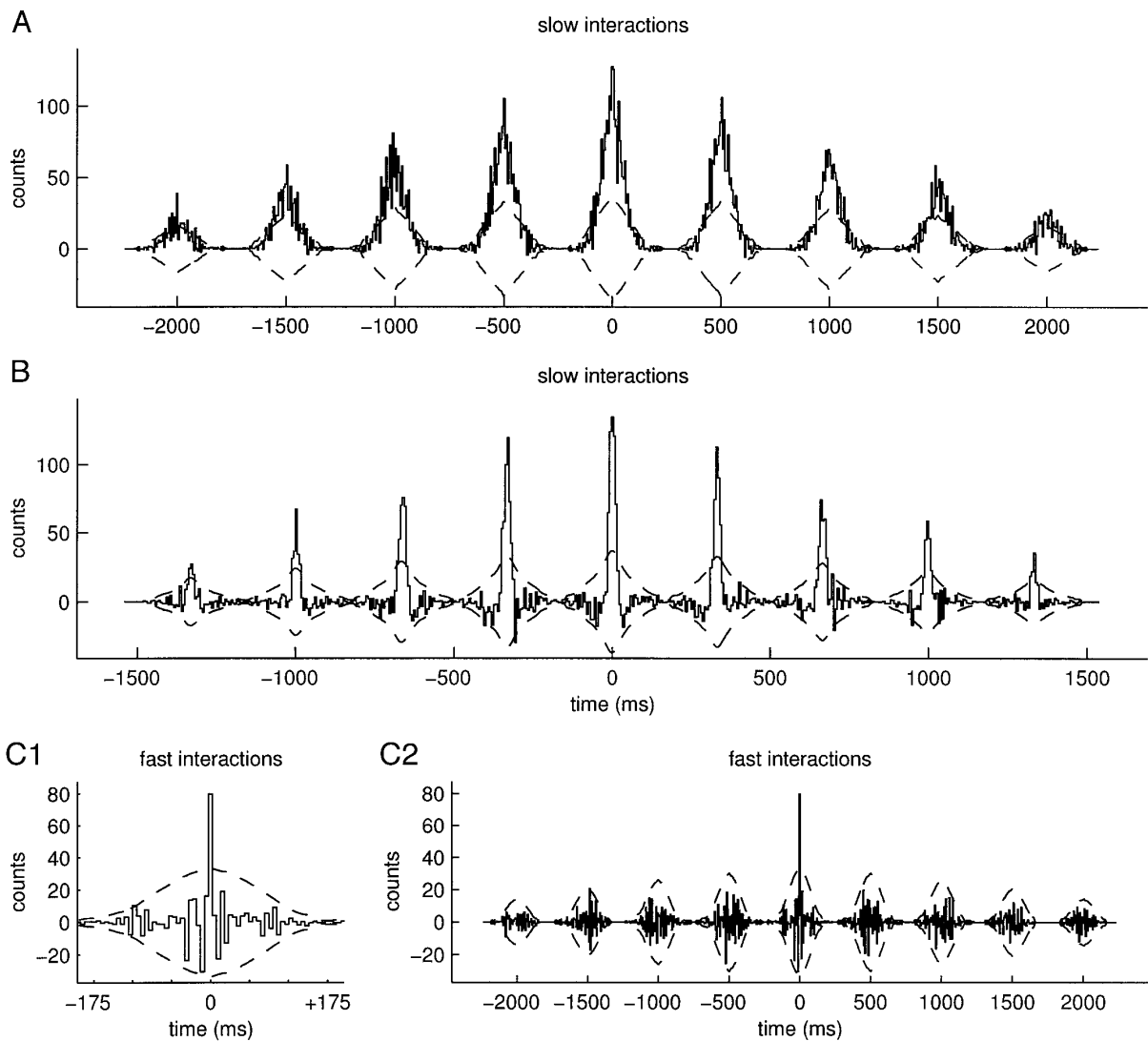


FIG. 3. Covariograms shown to their full extent, not clipped to a ± 175 -ms time window. Side peaks indicate an interaction with a timescale longer than the period of the sine-wave grating stimulus. *A*: covariogram of same spike trains of Fig. 2, *D1* and *D2*. *B*: covariogram of same spike trains of Fig. 2, *E1* and *E2*. *C*: covariogram from a variant of the model, different from that used for the other panels and figures; in this variant the resting potential was kept fixed, and the 2 LGN cells had a common ionotropic synaptic input in addition to their separate, independent RGC inputs.

covariograms with peaks similar in shape to the peak in the crosscovariogram (a condition true, but not shown here, for all panels of Fig. 2); and 3) significant positive integrals of the covariogram, which indicate positive covariations in mean firing rates during the experiment. Some quantitative methods to distinguish different contributions to a covariogram from each other were proposed (Brody 1998b; Friston 1995; Vaadia et al. 1995). Using the shift predictor instead of the shuffle corrector will ameliorate, but not eliminate, the effects of slow interactions.

The results depend on the nonlinear relationship between neuronal resting potential and stimulus response.² Other authors previously considered the effects of nonlinear input summation on covariograms; for example, Melssen and Ep-

ping (1987) showed that two different covariograms, each taken during different steady-state conditions, can lead to different estimates of the magnitude of a constant, existing, synaptic connectivity. This study extends that observation by 1) showing that covariations in neuronal states during trials taken for a single covariogram can lead to erroneous conclusions regarding the very presence of a neuronal connectivity (a possibility briefly mentioned, but not studied, by Aertsen et al. 1989) and 2) by demonstrating the strong modulatory effects that PSTHs can have on broad covariogram peaks. In general, a simple yet extremely important point to remember about covariograms is that significant peaks in them do indicate, very reliably, departure from independent firing of two cells; however, spike synchronization (suggestive of a synaptic connection) is only one of many ways to depart from independence.

Thanks to J. Hopfield and E. Winfree for discussion and comments on

² Note that even the simplest model, a leaky integrate-and-fire neuron, will show a nonlinear relationship between resting potential and stimulus response. The nonlinearity is more complex for LGN cells.

the manuscript, S. Manajan and S. Roweis for discussion, R. Romo and E. Salinas for comments on the manuscript, and J.-M. Alonso and R. C. Reid for generous sharing of RGC data. The simulator program used here, together with the scripts necessary to reproduce the figures in the paper, can be found at either <http://www.cns.caltech.edu/~carlos/programs/lgn> or <http://sonabend.ifisiot.unam.mx/~carlos/programs/lgn>.

Received 31 March 1998; accepted in final form 11 August 1998.

NOTE ADDED IN PROOF

A different model of the same data has appeared recently (Kirkland and Gerstein 1998). However, it explains only one of the three covariogram shapes, that of the type shown in Fig. 2E2. Furthermore, additional extensions of considerable complexity are required if the model is to account for the slow correlations time-scale found in the data (Kirkland 1998).

REFERENCES

- AERTSEN, A.M.H.J., GERSTEIN, G. L., HABIB, M. K., AND PALM, G. Dynamics of neuronal firing correlation—modulation of effective connectivity. *J. Neurophysiol.* 61: 900–917, 1989.
- BRODY, C. D. *Analysis and Modeling of Spike Train Correlations in the Lateral Geniculate Nucleus* (Ph.D. thesis), Caltech.[Online] [http://www.cns.caltech.edu/~carlos/thesis\[1997\]](http://www.cns.caltech.edu/~carlos/thesis[1997]).
- BRODY, C. D. Correlations without synchrony. *Neural Comput.* In press, 1998a.
- BRODY, C. D. Disambiguating different covariation types. *Neural Comput.* In press, 1998b.
- FRISTON, K. J. Neuronal transients. *Proc. R. Soc. Lond. B Biol. Sci.* 261: 401–405, 1995.
- GODWIN, D. W., VAUGHAN, J. W., AND SHERMAN, S. M. Metabotropic glutamate receptors switch visual response-mode of lateral geniculate-nucleus cells from burst to tonic. *J. Neurophysiol.* 76: 1800–1816, 1996.
- HUGUENARD, J. R. AND MCCORMICK, D. A. Simulation of the currents involved in rhythmic oscillations in thalamic relay neurons. *J. Neurophysiol.* 68: 1373–1383, 1992.
- JAHNSEN, H. AND LLINAS, R. Ionic basis for the electroresponsiveness and oscillatory properties of guinea pig thalamic neurons in vitro. *J. Physiol. (Lond.)* 349: 227–247, 1984.
- KIRKLAND, K. L. *Physiologically Based Simulations and Models of Feedback in the Visual System* (PhD thesis). Philadelphia, PA: University of Pennsylvania, 1998.
- KIRKLAND, K. L. AND GERSTEIN, G. L. A model of cortically induced synchronization in the lateral geniculate nucleus of the cat—a role for low-threshold calcium channels. *Vision Res.* 38: 2007–2022, 1998.
- MCCORMICK, D. A. AND HUGUENARD, J. R. A model of the electrophysiological properties of thalamocortical relay neurons. *J. Neurophysiol.* 68: 1384–1400, 1992.
- MCCORMICK, D. A. AND von KROSIGK, M. Corticothalamic activation modulates thalamic firing through glutamate metabotropic receptors. *Proc. Natl. Acad. Sci. USA* 89: 2774–2778, 1992.
- MELSSSEN, W. J. AND EPPING, W.J.M. Detection and estimation of neuronal connectivity based on cross-correlation analysis. *Biol. Cybern.* 57: 403–414, 1987.
- MONTERO, V. M. A quantitative study of synaptic contacts on interneurons and relay cells of the cat lateral geniculate nucleus. *Exp. Brain Res.* 86: 257–270, 1991.
- MUKHERJEE, P. AND KAPLAN, E. Dynamics of neurons in the cat lateral geniculate nucleus—in vivo electrophysiology and computational modeling. *J. Neurophysiol.* 74: 1222–1243, 1995.
- MUKHERJEE, P., OZAKI, T., AND KAPLAN, E. What controls the transfer of information through the LGN? *Soc. Neurosci. Abstr.* 21: 657, 1995.
- MURPHY, P. C. AND SILLITO, A. M. Functional morphology of the feedback pathway from area 17 of the cat visual cortex to the lateral geniculate nucleus. *J. Neurosci.* 16: 1180–1192, 1996.
- PALM, G., AERTSEN, A.M.H.J., AND GERSTEIN, G. L. On the significance of correlations among neuronal spike trains. *Biol. Cybern.* 59: 1–11, 1988.
- PERKEL, D. H., GERSTEIN, G. L., AND MOORE, G. P. Neuronal spike trains and stochastic point processes. II. simultaneous spike trains. *Biophys. J.* 7: 419–440, 1967.
- PRESS, W., TEUKOLSKY, S. A., VETTERING, W. T., AND FLANNERY, B. P. *Numerical Recipes in C* (2nd ed.). Cambridge, UK: Cambridge Univ. Press, 1992, p. 734–737.
- SHERMAN, S. M. AND GUILLERY, R. W. Functional organization of thalamocortical relays. *J. Neurophysiol.* 76: 1367–1395, 1996.
- SILLITO, A. M., JONES, H. E., GERSTEIN, G. L., AND WEST, D. C. Feature-linked synchronization of thalamic relay cell firing induced by feedback from the visual cortex. *Nature* 369: 479–482, 1994.
- UHLRICH, D. J., TAMAMAKI, N., MURPHY, P. C., AND SHERMAN, S. M. Effects of brain-stem parabrachial activation on receptive field properties of cells in the cats lateral geniculate nucleus. *J. Neurophysiol.* 73: 2428–2447, 1995.
- VAADIA, E., AERTSEN, A., AND NELKEN, I. 'Dynamics of neuronal interactions' cannot be explained by 'neuronal transients'. *Proc. R. Soc. Lond. B Biol. Sci.* 261: 407–410, 1995.